Weather & Climate of HD 189733b

Agol, Cowan* et al. submitted to ApJ

*at this meeting

Introduction: We analyze 7 transits and 7 eclipses of the hot Jupiter HD 189733b, obtained using the 8 micron IRAC instrument aboard *Spitzer*. The two principal goals of the study were 1) measure transit timing variations (TTV), hence constraining the presence of terrestrial planets in the system, and 2) measure the variability in eclipse depth, hence constraining weather variations on the planet.

Conclusions: We present best practices for reducing *Spitzer* 8 micron subarray data, including centroiding and ramp-correction. The system does not exhibit TTV (ruling out Mars-mass planets in mean-motion resonance) or eclipse depth variability (< 2.7% variations in day-side brightness). Unexpectedly, our stacked secondary eclipse observations are sufficiently precise to create the first eclipse map of a planet, which agrees quite nicely with the first phase function map of a planet. The position of its primary hotspot indicates that HD 189733b has an eastward equatorial jet stream with an advective timescale comparable to the radiative timescale, at the 8 micron photosphere.

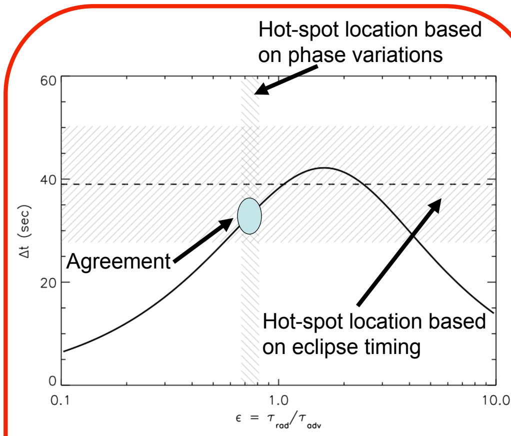

Figure 3: The basic eclipse fitting assumes that the planet has a uniform day-side; if the day-side is not uniform, the shape of ingress and egress, as well as the time of eclipse, may change (Williams et al. 2006). The solid line shows the expected eclipse timing offset as a function of the planet's advective efficiency, τ_{rad}/τ_{adv} (Cowan 2009). The observed delay is consistent with the hot-spot position as determined from thermal phase variations (Figure 4).

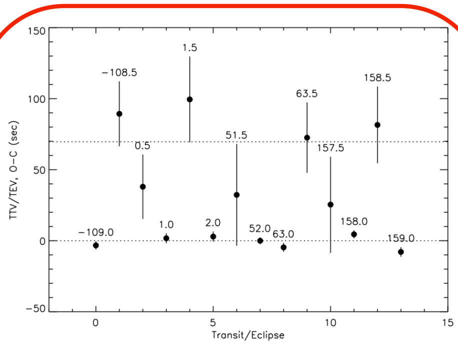

Figure 1: The transit times (w/ small error bars) and eclipse times (w/ larger error bars) are consistent with constant ephemerides (ie: both dotted lines are horizontal). This leads to constraints on additional planets in this system (Figure 2). However, the eclipses occur about 70 seconds later than one would predict based on the transit times. While 30 seconds of this delay can be explained by light travel time, the remaining delay can be accounted for by the eastward advection of the planet's primary hotspot (Figure 3).

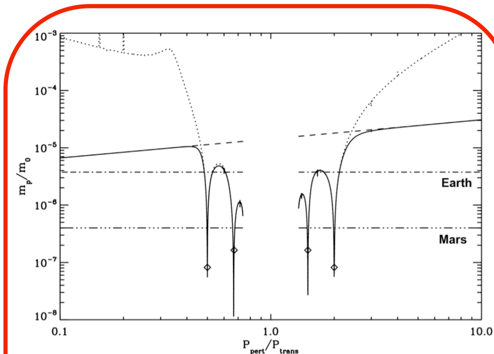

Figure 2: The lack of observed transit timing variations (TTV) in this system places stringent constraints on the mass of any additional planet in this system (solid black line). The dashed line shows the best constraint from radial velocity (RV) monitoring of the system. The solid line shows the best constraint combining RV and TTV. Mars-mass planets are excluded in mean-motion resonance. (Agol et al. 2005, Steffen & Agol 2005)

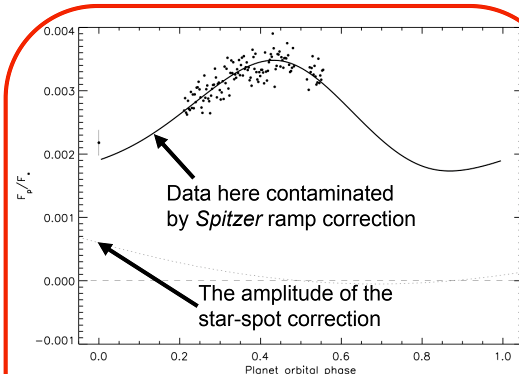

Figure 4: The dots show the thermal phase variations of Knutson et al. (2007). The black line shows the best-fit phase variation using the epsilon model of Cowan (2009). The dotted and dashed lines show the effect of star-spots, which we have corrected for.

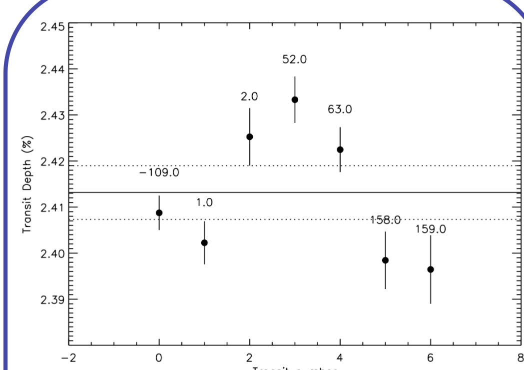

Figure 5: Variations in transit depth. The solid line shows the mean transit depth; the dotted lines show +/- 1σ scatter. This variability sets the limit on non-simultaneous transit spectroscopy.

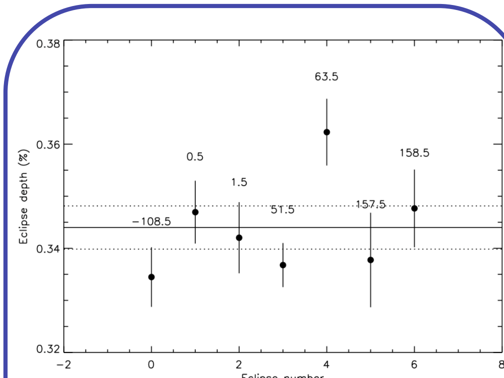

Figure 6: Variations in eclipse depth. The solid line shows the mean transit depth; the dotted lines show +/- 1σ scatter. We use a toy model to put this level of variability in perspective in Figure 7.

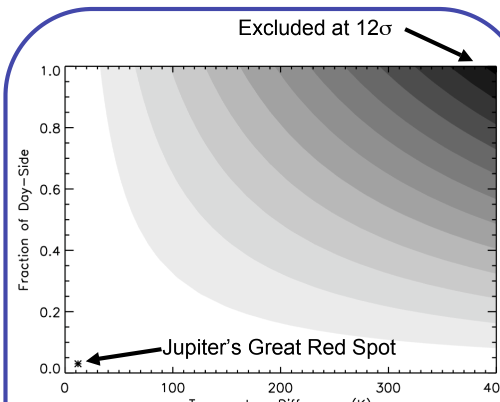

Figure 7: Our stringent upper-limit on the day-side variability of HD 189733b (< 2.7%) is put in perspective by considering the most obvious "storm" that could appear or dissipate during the course of our observations.